Inorganic Chemistry

Article

Photodriven Electron and Energy Transfer from a Light-Harvesting Metallodendrimer

Daniel S. Tyson, Charles R. Luman, and Felix N. Castellano*

Department of Chemistry and Center for Photochemical Sciences, Bowling Green State University, Bowling Green, Ohio 43403

Intermolecular electron and energy transfer from a light-harvesting metallodendrimer [Ru{bpy(C-450)$_4$}$_3$]$^{2+}$, where bpy(C-450)$_4$ is a 2,2′-bipyridine derivative containing 4 coumarin-450 units connected together through aryl ether linkages, is observed in acetonitrile solutions at room temperature. The model complex [Ru(dmb)$_3$]$^{2+}$, where dmb is 4,4′-dimethyl-2,2′-bipyridine, is included for quantitative comparison. The excited states of both compounds are metal-to-ligand charge transfer in nature and participate in excited-state electron and triplet energy transfer processes. Quenching constants were determined from luminescence and time-resolved absorption experiments at constant ionic strength. [Ru{bpy(C-450)$_4$}$_3$]$^{2+}$ displays significantly slower quenching rates to molecular oxygen and methyl viologen relative to the other processes investigated. Triplet energy transfer from [Ru{bpy(C-450)$_4$}$_3$]$^{2+}$ to 9-methylanthracene is quantitatively indistinguishable from [Ru(dmb)$_3$]$^{2+}$ while reductive electron transfer from phenothiazine was slightly faster in the former. With the exception of dioxygen quenching, our results indicate that the current dendritic structure is ineffective in shielding the core from bimolecular electron and triplet energy transfer reactions. Electrochemical measurements of [Ru{bpy(C-450)$_4$}$_3$]$^{2+}$ reveal irreversible oxidative processes at potentials slightly negative to the Ru(III/II) potential that are assigned to oxidations in the dendritic structure. Excited-state oxidative electron-transfer reactions facilitate this process resulting in the reduction of ground-state Ru(III) to Ru(II) and the trapping of the methyl viologen radical cation (MV$^{\bullet+}$) when methyl viologen serves as the quencher. This process generates a minimum of 9 MV$^{\bullet+}$'s for every [Ru{bpy(C-450)$_4$}$_3$]$^{2+}$ molecule and disassembles the metallodendrimer, resulting in the production of a [Ru(dmb)$_3$]$^{2+}$-like species and "free" C-450-like dyes.

Introduction

There continues to be increasing interest in the properties of dendritic structures that contain photo- and/or redox-active units. This curiosity stems from the possibility of generating well-defined macromolecules that can perform useful functions. In terms of metallodendrimers, many new structures have been developed that possess unique and potentially useful photophysical, photochemical, and electrochemical properties.[1-11] One particularly intriguing class of metallo-

dendrimers contains a single [Ru(bpy)$_3$]$^{2+}$ core (bpy = 2,2′-bipyridine) surrounded by a covalently attached dendrimer framework of organic composition.[9,10] Such a structural arrangement permits the evaluation of bimolecular electron- and energy-transfer reactions that can take place through the

* To whom correspondence should be addressed. Fax: (419) 372-9809. E-mail: castell@bgnet.bgsu.edu.

(1) Balzani, V.; Campagna, S.; Denti, G.; Juris, A.; Serroni, S.; Venturi, M. *Acc. Chem. Res.* **1998**, *31*, 26.
(2) Balzani, V.; Ceroni, P.; Juris, A.; Venturi, M.; Campagna, S.; Puntoriero, F.; Serroni, S. *Coord. Chem. Rev.* **2001**, *219–221*, 545.
(3) Gorman, C. *Adv. Mater.* **1998**, *10*, 295.
(4) (a) Jin, R.-H.; Aida, T.; Inoue, S. *J. Chem. Soc., Chem. Commun.* **1993**, 1260. (b) Sadamoto, R.; Tomioka, N.; Aida. *J. Am. Chem. Soc.* **1996**, *118*, 3978.
(5) Kimura, M.; Nakada, K.; Yamaguchi, Y.; Hanabusa, K.; Shirai, H.; Kobayashi, N. *Chem. Commun.* **1997**, 1215.
(6) Rajesh, C. S.; Capitosti, G. J.; Cramer, S. J.; Modarelli, D. A. *J. Phys. Chem. B* **2001**, *105*, 10175.
(7) (a) Constable, E. C. *Chem. Commun.* **1997**, 1073. (b) Constable, E. C.; Housecroft, C. E.; Cattalini, M.; Phillips, D. *New. J. Chem.* **1998**, *22*, 193.
(8) (a) Serroni, S.; Juris, A.; Venturi, M.; Campagna, S.; Resino, I. R.; Denti, G.; Credi, A.; Balzani, V. *J. Mater. Chem.* **1997**, *7*, 1227. (b) Venturi, M.; Serroni, S.; Juris, A.; Campagna, S.; Balzani, V. *Top. Curr. Chem.* **1998**, *197*, 193. (c) Maracaccio, M.; Paolucci, F.; Paradisi, C.; Roffia, S.; Fontanesi, C.; Yellowless, L. J.; Serroni, S.; Campagna, S.; Denti, G.; Balzani, V. *J. Am. Chem. Soc.* **1999**, *121*, 10081.
(9) (a) Issberner, J.; Vogtle, F.; De Cola, L.; Balzani, V. *Chem.—Eur. J.* **1997**, *3*, 706. (b) Plevoets, M.; Vögtle, F.; De Cola, L.; Balzani, V. *New J. Chem.* **1999**, *23*, 63. (c) Vögtle, F.; Plevoets, M.; Nieger, M.; Azzellini, G. C.; Credi, A.; De Cola, L.; De Marchis, V.; Venturi, M.; Balzani, V. *J. Am. Chem. Soc.* **1999**, *121*, 6290.
(10) Zhou, X.; Tyson, D. S.; Castellano, F. N. *Angew. Chem., Int. Ed.* **2000**, *39*, 4301.

dendritic architecture. Although this geometric assembly offers the possibility to modulate bimolecular electron- and energy-transfer rates, important toward the goal of realizing molecular control of intermolecular charge-transfer processes,[12–14] only a handful of studies have explored this possibility.[3,4,6,9,15] We note that there has also been some attention devoted to the use of dendrimers as supramolecular host environments for the assembly of Ru(II) polypyridine complexes with several types of quenchers.[16]

This work investigates photoinduced electron and energy transfer following visible excitation of a light-harvesting dendrimer containing a Ru(II) diimine core, [Ru{bpy(C-450)$_4$}$_3$]$^{2+}$,[10] where bpy(C-450)$_4$ is a coumarin-450-functionalized 2,2′-bipyridine ligand. [Ru(dmb)$_3$]$^{2+}$ (dmb = 4,4′-dimethyl-2,2′-bipyridine) served as a "naked" model system for the dendritic structure, and all experiments performed on each metal complex were run in parallel. Specifically, we measured the bimolecular quenching rates of dioxygen, 9-methylanthracene (triplet energy transfer), phenothiazine (reductive quenching), and methyl viologen (oxidative quenching) in CH$_3$CN solutions containing 50 mM tetrabutylammonium hexafluorophosphate, using 3 independent experimental techniques. In the case of reductive quenching with phenothiazine, charge recombination rates were measured by flash photolysis. Excited-state oxidative quenching resulted in the production of permanent photochemical products, precluding the evaluation of charge recombination rates in those systems. With the exception of dioxygen quenching, our results illustrate that the current first generation light-harvesting dendrimer behaves much like an exposed structure, where bimolecular electron- and energy-transfer rates are largely governed by the exothermicity of the respective process.

Experimental Section

Reagents. Phenothiazine (PTZ), 9-methylanthracene (MeAn), and tetrabutylammonium hexafluorophosphate (TBAPF$_6$) were obtained from Aldrich and used as received. Methyl viologen (MV^{2+}) dichloride and benzyl viologen (BV^{2+}) dichloride (Aldrich) were converted into their corresponding hexafluorophosphate salts by metathesis with NH$_4$PF$_6$ (Aldrich) in water. HPLC grade acetonitrile (CH$_3$CN) was purchased from Fisher and used without further purification.

Preparations. The light-harvesting dendrimer, [Ru{bpy(C-450)$_4$}$_3$](PF$_6$)$_2$, and corresponding model complex, [Ru(dmb)$_3$]-
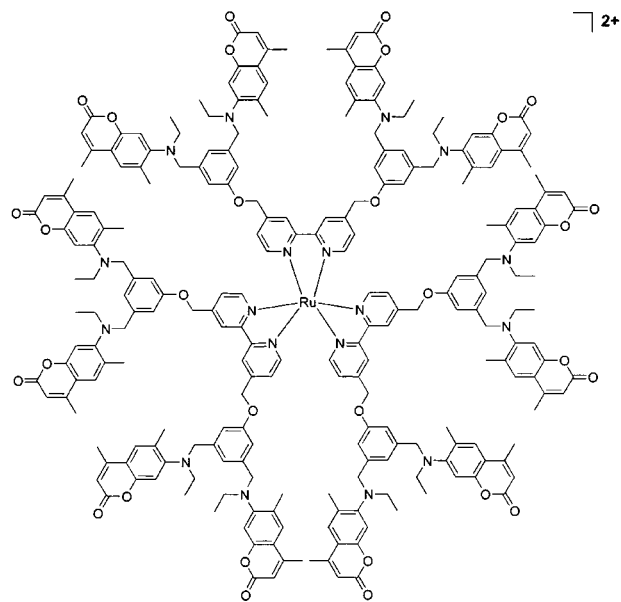
[Ru{bpy(C-450)$_4$}$_3$]$^{2+}$
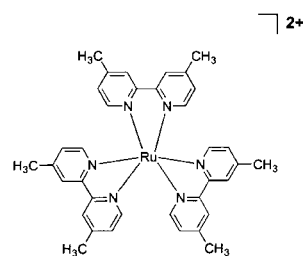
[Ru(dmb)$_3$]$^{2+}$

(PF$_6$)$_2$, were available from previous studies.[10,17] These complexes were purified by column chromatography on Sephadex LH-20 and precipitated by addition of NH$_4$PF$_6$(aq) to concentrated CH$_3$CN solutions. Purity was confirmed by analytical reversed-phase HPLC and FAB-MS. The oxidized model complex, [Ru(dmb)$_3$]$^{3+}$, was prepared through chemical oxidation of [Ru(dmb)$_3$]Cl$_2$.[18,19] This chloride salt was prepared by reacting the PF$_6^-$ salt with tetraethylammonium chloride in acetone.

Physical Measurements. All steady-state and time-resolved spectroscopic experiments have been described in detail elsewhere.[10,17,20] Excited-state absorption spectra and decay kinetics were obtained using the unfocused second harmonic provided by a Continuum Surelite I Nd:YAG laser (532 nm, 5–7 ns fwhm). All room-temperature luminescence and time-resolved absorbance measurements were performed in argon-saturated CH$_3$CN solutions. The 77 K luminescence spectra were obtained in 4:1 EtOH/MeOH glasses with samples contained in 5 mm NMR tubes, suspended in a quartz-tipped finger LN$_2$ dewar. Cyclic voltammetry was performed in a one-compartment cell using a three-electrode arrangement incorporating a Pt disk working electrode, a Pt wire auxiliary electrode, and a Ag/AgCl (3 M KCl) reference electrode. Electro-

(11) (a) Marvaud, V.; Astruc, D. *Chem. Commun.* **1997**, 773. (b) Takada, K.; Diaz, D. J.; Abruna, H. D.; Cuadrado, I.; Casado, C.; Alonso, B.; Moran, M.; Losada, J. *J. Am. Chem. Soc.* **1997**, *119*, 10763. (c) Storrier, G. D.; Takada, K.; Abruna, H. D. *Langmuir* **1999**, *15*, 872. (d) Zhou, M.; Rooves, J. *Macromolecules* **2001**, *34*, 244.

(12) Olmsted, J., III; McClanahan, S. F.; Danielson, E.; Younathan, J. N.; Meyer, T. J. *J. Am. Chem. Soc.* **1987**, *109*, 3297.

(13) Rabani, J.; Sasson, R. E. *J. Photochem.* **1985**, *29*, 7.

(14) Stipkala, J. M.; Castellano, F. N.; Heimer, T. A.; Kelly, C. A.; Livi, K. J. T.; Meyer, G. J. *Chem. Mater.* **1997**, *9*, 2341.

(15) Devadoss, C.; Bharathi, P.; Moore, J. S. *Macromolecules* **1998**, *31*, 8091.

(16) (a) Moreno-Bondi, M. C.; Orellana, G.; Turro, N. J.; Tomalia, D. A. *Macromolecules* **1990**, *23*, 910. (b) Turro, N. J.; Barton, J. K.; Tomalia, D. A. *Acc. Chem. Res.* **1991**, *24*, 332. (c) Turro, C.; Niu, S.; Bossmann, S. H.; Tomalia, D. A.; Turro, N. J. *J. Phys. Chem.* **1995**, *99*, 5512. (d) ben-Avraham, D.; Schulman, L. S.; Bossmann, S. H.; Turro, C.; Turro, N. J. *J. Phys. Chem. B* **1998**, *102*, 5088.

(17) Tyson, D. S.; Castellano, F. N. *J. Phys. Chem. A* **1999**, *103*, 10955.

(18) Ghosh, P. K.; Brunschwig, B. S.; Chou, C.; Creutz, C.; Sutin, N. *J. Am. Chem. Soc.* **1984**, *106*, 4772.

(19) Nazeeruddin, M. K.; Zakeeruddin, S. M.; Kalyanasundaram, K. *J. Phys. Chem.* **1993**, *97*, 9607.

(20) (a) Tyson, D. S.; Luman, C. R.; Zhou, X.; Castellano, F. N. *Inorg. Chem.* **2001**, *40*, 4063. (b) Tyson, D. S.; Henbest, K. B.; Bialecki, J.; Castellano, F. N. *J. Phys. Chem. A* **2001**, *105*, 8154.

chemical experiments were performed in conjunction with a BAS Epsilon controller interfaced with a Pentium PC. Under typical experimental conditions (deaerated CH_3CN with 0.1 M $(TBA)PF_6$ supporting electrolyte), the ferrocene/ferrocenium couple was determined to be +0.43 V vs Ag/AgCl. Reversed-phase HPLC analysis was performed on a semipreparative C-18 column (YMC ODS-A, S-5 μm 120 Å, 250 × 10 mm i. d.) using a two-pump system (Waters model 515) to generate linear gradients of CH_3-CN/H_2O (50/50 initial, 2% per min gradient to 100/0). The HPLC system was equipped with a Waters model 994 diode array detector.

Quenching Experiments. For all quenching experiments, stock solutions of the appropriate Ru(II) complex were prepared in CH_3-CN containing 50 mM $(TBA)PF_6$. Samples of known quencher concentration were prepared by adding an appropriate amount of solid quencher to 5 or 10 mL volumetric flasks containing either [Ru{bpy(C-450)$_4$}$_3$]$^{2+}$ or [Ru(dmb)$_3$]$^{2+}$ stock solutions. Samples were deaerated by a stream of CH_3CN−saturated argon for at least 20 min following transfer to anaerobic quartz cells (1 cm path length) and maintained under a blanket of argon. Static lumines-cence spectra, luminescence decay profiles, and excited-state absorption spectra were then collected for each sample. UV−vis spectra were taken before and after each experiment to monitor potential buildup of photochemical products. In the [Ru(dmb)$_3$]$^{2+}$ model system, there was no evidence of any photochemistry under all experimental conditions. Similarly for [Ru{bpy(C-450)$_4$}$_3$]$^{2+}$, triplet energy transfer and reductive excited-state electron transfer did not result in the accumulation of photochemical products. However, in the case of oxidative excited-state electron transfer, visible excitation of [Ru{bpy(C-450)$_4$}$_3$]$^{2+}$ generated permanent photochemical products. This photochemistry was explored in detail with 460 nm excitation (450 W Xe lamp/monochromator) using 10 mM MV^{2+} and BV^{2+}.

In all samples, quenching constants (k_q) were independently evaluated using both luminescence and time-resolved absorption experiments. Addition of quenchers to the Ru(II) compounds resulted in concentration dependent luminescence intensity and lifetime quenching. This bimolecular quenching was well modeled by Stern−Volmer kinetics, eq 1,[21] where I_0 is the integrated MLCT emission intensity in the absence of quencher, τ_0 is the excited-state lifetime in the absence of quencher, I and τ are the corresponding values in the presence of quencher, k_q is the bimolecular quenching rate constant, and [Q] is the molar concen-tration of the quencher. Kinetic analysis of the absorption transients associated with photogenerated electron or energy transfer products yielded pseudo-first-order rate constants (k_{obs}). These rate constants were converted into second-order rate constants (k_q) by using the quencher concentrations present in pseudo-first-order excess, $k_{obs} = k_q[Q]$.

$$I_0/I = \tau_0/\tau = 1 + k_q\tau_0[Q] \qquad (1)$$

Results and Discussion

Photophysical and Light-Harvesting Properties. The absorption and uncorrected room-temperature emission spec-tra of [Ru{bpy(C-450)$_4$}$_3$]$^{2+}$ and the model complex [Ru-(dmb)$_3$]$^{2+}$ are presented in Figure 1. Both complexes possess typical MLCT absorption features in the visible. The light-harvesting dendrimer displays increased absorption near 343 nm largely attributed to 12 covalently attached coumarin-
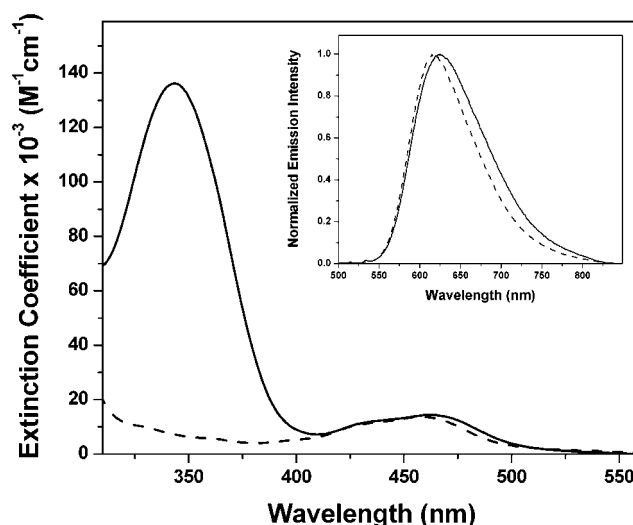
(21) Lakowicz, J. R. *Principles of Fluorescence Spectroscopy*, 2nd ed.; Kluwer Academic/Plenum Publishers: New York, 1999.

Figure 1. Electronic spectra of [Ru{bpy(C-450)$_4$}$_3$]$^{2+}$ (solid line) and [Ru-(dmb)$_3$]$^{2+}$ (dashed line) in CH_3CN at room temperature. Inset: Uncorrected emission spectra of [Ru{bpy(C-450)$_4$}$_3$]$^{2+}$ (solid line) and [Ru(dmb)$_3$]$^{2+}$ (dashed line) in CH_3CN obtained with 460 ± 2 nm excitation.

450 antenna chromophores. The emission spectrum of [Ru-{bpy(C-450)$_4$}$_3$]$^{2+}$ (625 nm) is slightly red shifted compared to that of [Ru(dmb)$_3$]$^{2+}$ (622 nm). The emission quantum yields of [Ru{bpy(C-450)$_4$}$_3$]$^{2+}$ and [Ru(dmb)$_3$]$^{2+}$ in CH_3-CN are also similar, 0.073 ± 0.007 and 0.071 ± 0.008, respectively. The energy of the lowest metal-to-ligand charge transfer (MLCT) excited states for [Ru{bpy(C-450)$_4$}$_3$]$^{2+}$ and [Ru(dmb)$_3$]$^{2+}$ were estimated by their emission maxima at 77 K, 16 750 cm^{-1} (2.08 eV) and 17 000 cm^{-1} (2.11 eV), respectively. It should be noted that our estimated [Ru-(dmb)$_3$]$^{2+}$ E_{00} energy is similar to that obtained from emission spectral fitting (17 310 cm^{-1}).[22] Therefore, the 77 K estimates of the E_{00} energies provide reasonable approximations in lieu of Franck−Condon analysis. The luminescence character-istics exhibited by the two metal complexes are consistent with that of MLCT excited states of Ru(II)−diimine com-pounds. The excited states of each molecule decay with first-order kinetics, displaying similar lifetimes in deaerated CH_3CN (1.04 μs and 875 ns, respectively). Importantly, the dendrimer system retains the favorable properties of the core (emission quantum yield and excited-state lifetime) with the added advantage of increased molar extinction coefficient in the UV region. We have previously detailed the light-harvesting and intramolecular energy transfer behavior of the [Ru{bpy(C-450)$_4$}$_3$]$^{2+}$ dendritic system.[10]

Figure 2 displays the excited-state absorption difference spectra for [Ru(dmb)$_3$]$^{2+}$ and [Ru{bpy(C-450)$_4$}$_3$]$^{2+}$ in CH_3-CN obtained at a variety of delay times following a 532 nm laser pulse. In both compounds a clear isosbestic point is observed near 400 nm. The positive absorption features centered near 370 nm are assigned to the reduced dmb ligand in [Ru(dmb)$_3$]$^{2+*}$,[22] characteristic of the charge-transfer nature of the excited states. On the basis of their similarity, we assign the same feature in the [Ru{bpy(C-450)$_4$}$_3$]$^{2+*}$

(22) (a) Damrauer, N. H.; Boussie, T. R.; Devenney, M.; McCusker, J. K. *J. Am. Chem. Soc.* **1997**, *119*, 8253. (b) Damrauer, N. H.; McCusker, J. K. *J. Phys. Chem. A* **1999**, *103*, 8440.
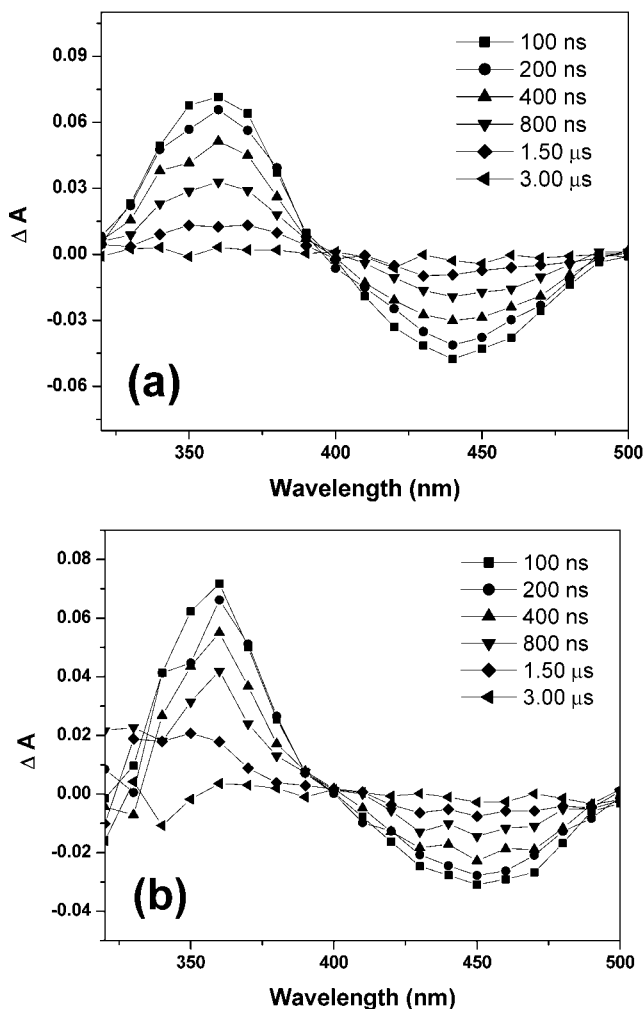
Figure 2. Excited-state absorption difference spectra for (a) $[Ru(dmb)_3]^{2+}$ and (b) $[Ru\{bpy(C-450)_4\}_3]^{2+}$ in deaerated CH_3CN recorded at various delay times following 532 nm pulsed excitation.

Table 1. Redox Potentials in CH_3CN^a

compd	$E_{1/2}$	$Ru^{3+/2+*\,f}$	$Ru^{2+/+*\,f}$
$[Ru(dmb)_3]^{2+}$	$+1.16^b$ $(-1.4)^c$	-0.95	$+0.71$
$[Ru\{bpy(C-450)_4\}_3]^{2+}$	$+1.33^{b,d}$ $(-1.2)^{c,e}$	-0.75	$+0.88$
$bpy(C-450)_4^{+/0}$	$+1.22^e$		
$MV^{2+/\bullet+}$	-0.38		
$BV^{2+/\bullet+}$	-0.31		
$PTZ^{\bullet+/0}$	$+0.64$		
$MeAn^{+/0}$	$+1.22$		
$C-450^{+/0}$	$+1.06^e$		

^{a} All ground-state potentials measured in 0.1 M $(TBA)PF_6$ in deaerated CH_3CN. Values given in V vs Ag/AgCl. The scan rate was 100 mV/s. ^{b} Ru(III/II) potential. ^{c} First observed ligand-based reduction. ^{d} Shoulder observed at $E_{pa} = +1.20$ V is attributed to oxidation in the $bpy(C-450)_4$ ligand. ^{e} Irreversible wave. ^{f} Excited-state potentials calculated as $E^{3+/2+*} = E^{3+/2+} - E_{00}$ and $E^{2+/+*} = E^{2+/+} + E_{00}$.

ligand $bpy(C-450)_4$ (+1.22 V), not surprising given their structural differences (secondary verses tertiary amine). In this study we will make use of the ternary amine structures to serve as the most appropriate model systems.

We do not possess sufficient amounts of $[Ru\{bpy(C-450)_4\}_3]^{2+}$ for proper quantitative electrochemical measurements. With the material on hand we were able to perform cyclic voltammetry measurements on a dilute sample, which was found to slowly decompose during the course of the experiments. The following data present these results and should be viewed with vigilance. $[Ru\{bpy(C-450)_4\}_3]^{2+}$ exhibits closely spaced irreversible oxidative processes that occur at potentials more positive than that of the metal-based oxidation in $[Ru(dmb)_3]^{2+}$. The first wave ($E_{pa} = +1.20$ V vs Ag/AgCl) is assigned to an irreversible oxidation in the ligand structure, consistent with that observed in the free ligand $(bpy(C-450)_4)$ at $+1.22$ V. The other process which is not completely reversible ($E_{pa} = +1.33$ V) is assigned as the Ru(III/II) potential. This shift of the Ru(III/II) potential to more positive potentials is consistent with that observed in other redox-active core metallodendrimers.[2,3,9] These oxidations result in decomposition of $[Ru\{bpy(C-450)_4\}_3]^{2+}$ over the course of several sweeps, generating a C-450-like blue emitting species, along with MLCT emitting species. We will discuss these processes later on as they are facilitated during bimolecular excited-state oxidative electron transfer. The reductive electrochemistry displayed by $[Ru\{bpy(C-450)_4\}_3]^{2+}$ was also quite complex, exhibiting multiple

transient spectrum to a dmb-like reduced ligand. The visible MLCT absorption bands are also bleached in the excited states of both molecules. These absorption features recover by a first-order process with kinetics that are in quantitative agreement with the emission intensity decays. The kinetics of $[Ru(dmb)_3]^{2+}$ are also in good agreement with the values reported in other studies.[17,22] Absorption wavelengths above 550 nm were not evaluated due to the strong orange to red luminescence exhibited by these complexes on the time scale of the experiment. Comparison of the features in the transient spectra leads us to conclude that direct population of the MLCT excited states in $[Ru\{bpy(C-450)_4\}_3]^{2+}$ does not appear to generate any transient species directly associated with the C-450 peripheral units.

Electrochemistry. Cyclic voltammetry measurements were performed on all compounds used in this study. These electrochemical data are collected in Table 1, reported against the Ag/AgCl reference. The data obtained for $[Ru(dmb)_3]^{2+}$, MeAn, MV^{2+}, BV^{2+}, and PTZ are consistent with that expected for each of those species in CH_3CN.[22-28] 4,7-Dimethyl-7-(ethylamino)coumarin (C-450) displays an irreversible oxidation at $+1.06$ V. The C-450 oxidation differs significantly from that observed in the C-450-containing
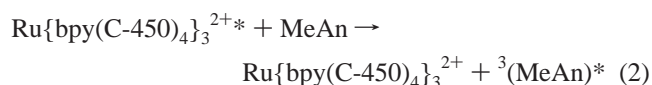
(23) (a) Bock, C. R.; Meyer, T. J.; Whitten, D. G. *J. Am. Chem. Soc.* **1974**, *96*, 4710. (b) Bock, C. R.; Connor, J. A.; Gutierrez, A. R.; Meyer, T. J.; Whitten, D. G.; Sullivan, B. P.; Nagle, J. K. *J. Am. Chem. Soc.* **1979**, *101*, 4815. (c) Chen, P.; Westmoreland, T. D.; Danielson, E.; Schanze, K. S.; Anthon, D.; Neveux, P. E., Jr.; Meyer, T. J. *Inorg. Chem.* **1987**, *26*, 1116. (d) Meyer, T. J. *Acc. Chem. Res.* **1989**, *22*, 163.
(24) Yonemoto, E. H.; Riley, R. L.; Kim, Y. I.; Atherton, S. J.; Schmehl, R. H.; Mallouk, T. E. *J. Am. Chem. Soc.* **1992**, *114*, 8081.
(25) (a) Elliott, C. M.; Freitag, R. A.; Blaney, D. D. *J. Am. Chem. Soc.* **1985**, *107*, 4647. (b) Larson, S. L.; Elliott, C. M.; Kelley, D. F. *Inorg. Chem.* **1996**, *35*, 2070.
(26) (a) Ohno, T.; Yoshimura, A.; Mataga, N. *J. Phys. Chem.* **1986**, *90*, 3295. (b) Ohno, T.; Yoshimura, A.; Mataga, N. *J. Phys. Chem.* **1990**, *94*, 4871.
(27) (a) Hoffman, M. Z. *J. Phys. Chem.* **1988**, *92*, 3458. (b) Ohno, T.; Yoshimura, A.; Prasad, D. R.; Hoffman, M. Z. *J. Phys. Chem.* **1991**, *95*, 4723.
(28) Chiorboli, C.; Indelli, M. T.; Scandola, M. A. R.; Scandola, F. *J. Phys. Chem.* **1988**, *92*, 156.

irreversible reductions, the first peak centered at -1.2 V. This reduction takes place at potentials substantially less negative than that observed in [Ru(dmb)$_3$]$^{2+}$. The shift of the first reduction potential to less negative potentials has also been observed in other Ru(II) metallodendrimer core materials.[2,3,9] Due to limited amounts of [Ru{bpy(C-450)$_4$}$_3$]$^{2+}$, no further attempts were made to study the reductive processes.

Taken together, the cyclic voltammetry data along with the 77 K luminescence data can be used to estimate the excited-state redox potentials in [Ru(dmb)$_3$]$^{2+}$ and [Ru{bpy-(C-450)$_4$}$_3$]$^{2+}$.[9,23–25] These values are listed in Table 1, and it should be noted that the values obtained for [Ru(dmb)$_3$]$^{2+}$ are in quantitative agreement with those previously reported.[25] Due to the uncertainty in the ground-state redox processes, the calculated excited-state potentials reported for [Ru{bpy(C-450)$_4$}$_3$]$^{2+}$ should be treated as crude estimates.

Oxygen Quenching. Ground-state molecular oxygen is a well-known quencher for the MLCT excited states of Ru(II) polypyridyl complexes.[2,9,10,29,30] The actual quenching mechanism is somewhat controversial as combinations of energy and electron-transfer pathways have been proposed.[30] The bimolecular quenching constants (k_q) for [Ru(dmb)$_3$]$^{2+}$ and [Ru{bpy(C-450)$_4$}$_3$]$^{2+}$ were determined to be 1.0×10^9 and 2.5×10^8 M^{-1} s^{-1}, respectively. These values were calculated from differences in excited-state lifetime measured in argon- and air-saturated CH$_3$CN. Similar to that observed in related Ru(II) metal–organic dendrimers, the peripheral units are potentially shielding the diffusion of molecular oxygen in the region immediately surrounding the photoexcited core, resulting in a smaller quenching rate than one would expect. However, we believe a lower solubility of dioxygen within the dendritic structure is most likely responsible for attenuation of the bimolecular rate constant. Under ambient, air-saturated conditions, the photophysical properties of [Ru{bpy-(C-450)$_4$}$_3$]$^{2+}$ can be considered slightly enhanced (longer excited-state lifetime and higher quantum yield) relative to the model complex, [Ru(dmb)$_3$]$^{2+}$. This suggests that dendritic architectures containing MLCT cores will be useful toward the design of luminescent photonic devices requiring long excited-state lifetimes.

Triplet Energy Transfer. 9-Methylanthracene (MeAn) served as a triplet energy-transfer quencher for the light-harvesting dendrimer and the model complex in this study. The excited-state quenching scheme displayed in eq 2 is written in terms of triplet state quenching of photoexcited [Ru{bpy(C-450)$_4$}$_3$]$^{2+}$*:[12,31]

$$\text{Ru\{bpy(C-450)}_4\}_3{}^{2+}* + \text{MeAn} \rightarrow$$
$$\text{Ru\{bpy(C-450)}_4\}_3{}^{2+} + {}^3(\text{MeAn})* \quad (2)$$

Pulsed laser excitation (532 nm) of MeAn solutions contain-

Table 2. Room-Temperature Quenching Rate Constants (M^{-1} s^{-1})^a

| compd	method	MV^{2+}	MeAn	PTZ	O$_2$
[Ru(dmb)$_3$]$^{2+}$	$\tau_{em}{}^b$	1.6×10^9	6.0×10^9	1.5×10^9	1.03×10^9
	$I_Q{}^c$	1.1×10^9	3.6×10^9	1.3×10^9	
	$\tau_{TA}{}^d$	3.1×10^9	5.6×10^9	1.7×10^9	
[Ru{bpy(C-450)$_4$}$_3$]$^{2+}$	$\tau_{em}{}^b$	3.1×10^8	4.3×10^9	3.7×10^9	2.5×10^8
	$I_Q{}^c$	2.7×10^8	2.9×10^9	2.4×10^9	
	$\tau_{TA}{}^d$		4.2×10^9	4.5×10^9	

^{a} Deaerated CH$_3$CN solutions containing 5×10^{-2} M (TBA)PF$_6$. Uncertainty in the quenching constants is $\pm 10\%$. ^{b} Indicates Stern–Volmer analysis of luminescence lifetime quenching. Lifetimes were single exponential at all concentrations reported. ^{c} Indicates Stern–Volmer analysis of luminescence intensity quenching using $\lambda_{ex} = 460$ nm. ^{d} Pseudo-first-order analysis of the kinetic growth of the absorption transients for each quencher as a function of quencher concentration.

ing either [Ru(dmb)$_3$]$^{2+}$ or [Ru{bpy(C-450)$_4$}$_3$]$^{2+}$ generated absorption transients consistent with the production of ^{3}(MeAn)*.[12,31,32] Following its sensitization, the decay of ^{3}(MeAn)* obeys first-order kinetics, regenerating the MeAn ground state in 36–113 and 35–46 μs for [Ru(dmb)$_3$]$^{2+}$ and [Ru{bpy(C-450)$_4$}$_3$]$^{2+}$, respectively. The observed decay kinetics of ^{3}MeAn* was dependent on the concentration of MeAn in the solution, consistent with observations made by other investigators in related systems.[32] The three k_q values calculated for the quenching of [Ru(dmb)$_3$]$^{2+}$* and [Ru{bpy-(C-450)$_4$}$_3$]$^{2+}$* by MeAn are summarized in Table 2. All three methods yielded consistent values for k_q (within experimental error) for each compound with only minor differences between [Ru(dmb)$_3$]$^{2+}$ and [Ru{bpy(C-450)$_4$}$_3$]$^{2+}$, the latter being smaller. The lack of any static quenching in the photoluminescence data combined with the absence of prompt transients in the flash photolysis experiments indicate that energy transfer is not a result of ground-state association between each metal complex and MeAn. Considering the fact that the MLCT triplet energies of [Ru(dmb)$_3$]$^{2+}$ and [Ru{bpy(C-450)$_4$}$_3$]$^{2+}$ are almost identical, it seems reasonable that the quenching constants would reflect this energetic proximity. However, the dioxygen quenching described above yields almost 1 order of magnitude difference in bimolecular quenching rate. It seems rather unlikely that the neutral MeAn species would be more accessible to the photoexcited core than O$_2$, although the data imply otherwise. The energy-transfer data support the notion that the current dendritic structure does not impede the interaction of MeAn with the core.

Reductive Quenching. PTZ was used as a quencher for both [Ru(dmb)$_3$]$^{2+}$* and [Ru{bpy(C-450)$_4$}$_3$]$^{2+}$*.[12,23c–d,25b,26] Reductive excited-state electron transfer takes place between [Ru{bpy(C-450)$_4$}$_3$]$^{2+}$* and PTZ according to eq 3. The presence of oxidized PTZ$^{+•}$ was readily determined from its distinct absorption transients in the visible.[12,26,33,34]

(29) (a) Demas, J. N.; Harris, E. W.; McBride, R. P. *J. Am. Chem. Soc.* **1977**, *99*, 3547. (b) Demas, J. N.; DeGraff, B. A. *Anal. Chem.* **1991**, *63*, 829A. (c) Demas, J. N.; DeGraff, B. A. *Coord. Chem. Rev.* **2001**, *211*, 317.

(30) (a) Mulazzani Q. G.; Sun, H.; Hoffman, M. Z.; Ford, W. E.; Rogers M. A. J. *J. Phys Chem.* **1994**, *98*, 1145. (b) Zhang, X.; Rodgers, M. A. J. *J. Phys. Chem.* **1995**, *99*, 12797.
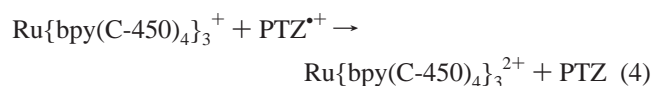
(31) (a) Johansen, O.; Mau, A.; Sasse, W. H. F. *Chem. Phys. Lett.* **1983**, *94*, 113. (b) Mau, A.; Johansen, O.; Sasse, W. H. F. *Photochem. Photobiol.* **1985**, *41*, 503.

(32) (a) Castellano, F. N.; Ruthkosky, M.; Meyer, G. J. *Inorg. Chem.* **1995**, *34*, 3. (b) Ruthkosky, M.; Castellano, F. N.; Meyer, G. J. *Inorg. Chem.* **1996**, *35*, 6406.

(33) Alkaitis, S. A.; Beck, G.; Grätzel, M. *J. Am. Chem. Soc.* **1975**, *97*, 5723.

(34) Argazzi, R.; Bignozzi, C. A.; Heimer, T. A.; Castellano, F. N.; Meyer, G. J. *J. Phys. Chem. B* **1997**, *101*, 2591.

Three k_q's for [Ru(dmb)$_3$]$^{2+}$ and [Ru{bpy(C-450)$_4$}$_3$]$^{2+}$ were calculated from the experimental data and are presented in Table 2. From all methods, the quenching constants for the dendritic species were consistently higher than those measured for the model complex. Considering the electrochemical potentials provided in Table 1, the driving force for electron transfer from PTZ to [Ru{bpy(C-450)$_4$}$_3$]$^{2+}$* is 160 mV greater than the same process for [Ru(dmb)$_3$]$^{2+}$*. We have performed a Marcus-type correlation using the current PTZ quenching data and [Ru(bpy)$_3$]$^{2+}$* literature data (see Supporting Information). Although several assumptions were used, this analysis illustrates that the differences in quenching rate constants can be completely accounted for by differences in driving force. Therefore, we conclude that the MLCT core must be readily accessible to collisions with PTZ and the dendritic structure does not impede this process, similar to what was observed for MeAn above. This is not completely surprising given the literature precedence in a related but larger Ru(II) metallodendrimer, where bimolecular reductive quenching by tetrathiafulvalene (TTF) was only attenuated by a factor of 2 relative to [Ru(bpy)$_3$]$^{2+}$.[2,9c]

$$Ru\{bpy(C\text{-}450)_4\}_3^{2+}* + PTZ \rightarrow$$
$$Ru\{bpy(C\text{-}450)_4\}_3^{+} + PTZ^{\bullet+} \quad (3)$$
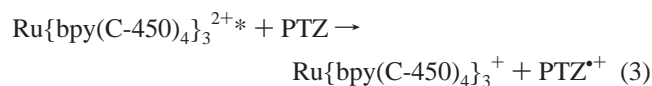
The charge recombination reaction involves [Ru{bpy(C-450)$_4$}$_3$]$^{+}$ and PTZ$^{+\bullet}$, depicted in eq 4.[26]

This recombination obeys second-order equal concentration kinetics yielding rate constants of $(1.8 \pm 0.1) \times 10^{10}$ M^{-1} s^{-1} for the [Ru(dmb)$_3$]$^{+}$/PTZ$^{\bullet+}$ pair and $(2.3 \pm 0.4) \times 10^{10}$ M^{-1} s^{-1} for the [Ru{bpy(C-450)$_4$}$_3$]$^{+}$/PTZ$^{+\bullet}$ pair. The measurement error reflects 8 independent transient absorption measurements taken at 514 nm. At 514 nm, $\epsilon(PTZ^{\bullet+}) = 7000$ M^{-1} cm^{-1} and ground-state bleaching of both metal complexes is negligible.[35] Both recombination reactions are highly exothermic and occur within experimental error of the diffusion limit in acetonitrile (1.9×10^{10} M^{-1} s^{-1}).[36] On the basis of the experimentally determined rate constants, it is clear that the dendrimer periphery has no influence upon the rate of the highly exothermic recombination reaction in [Ru{bpy(C-450)$_4$}$_3$]$^{2+}$. It should be noted that the hydrophobic nature of the PTZ molecule may potentially serve as a driving force for its incorporation into the dendritic structure, similar to its accumulation into micellar environments.[33]

$$Ru\{bpy(C\text{-}450)_4\}_3^{+} + PTZ^{\bullet+} \rightarrow$$
$$Ru\{bpy(C\text{-}450)_4\}_3^{2+} + PTZ \quad (4)$$

Oxidative Quenching. MV^{2+} was used as an oxidative quencher for both [Ru(dmb)$_3$]$^{2+}$* and [Ru{bpy(C-450)$_4$}$_3$]$^{2+}$*. Excited-state electron transfer takes place as shown in eq 5, yielding methyl viologen radical (MV$^{\bullet+}$) and the oxidized Ru(III) ground-state complex.[2,23,24,25a,27,28]

Figure 3. Absorption difference spectrum generated by excitation of [Ru{bpy(C-450)$_4$}$_3$]$^{2+}$ (3.7 μM) at 460 nm in the presence of 10 mM MV^{2+}. The reagents were dissolved in deaerated CH$_3$CN containing 50 mM (TBA)-PF$_6$ with 32.7 μM MV$^{\bullet+}$ being produced in this particular experiment.

The calculated k_q's for [Ru(dmb)$_3$]$^{2+}$ and [Ru{bpy(C-450)$_4$}$_3$]$^{2+}$ are presented in Table 2. In general, there is a lowering of the quenching constant for the dendritic species by almost 1 order of magnitude relative to the [Ru(dmb)$_3$]$^{2+}$*/ MV^{2+} reaction. We performed the same Marcus-type correlation with the oxidative quenching data as we did with PTZ earlier. Comparison of our data with literature values reveals that the differences observed in our electron-transfer rates can be largely accounted for by differences in driving force (see Supporting Information). At first glance this may seem peculiar; however, the excited-state oxidation potentials of the model complex and metallodendrimer differ by 200 mV and can account for most of the rate difference. A slight attenuation in rate constant in the dendrimer may be related to solubility of MV^{2+} in the vicinity of the dendritic structure, but we emphasize that such an effect represents only a minor contribution to the observed rate constants.

$$Ru\{bpy(C\text{-}450)_4\}_3^{2+}* + MV^{2+} \rightarrow$$
$$Ru\{bpy(C\text{-}450)_4\}_3^{3+} + MV^{\bullet+} \quad (5)$$
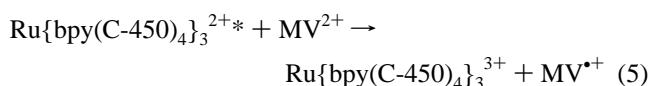
The use of MV^{2+} as an oxidative quencher for [Ru{bpy(C-450)$_4$}$_3$]$^{2+}$ led to long-term trapping of the methyl viologen radical cation, Figure 3. Initial experiments exhibited a dramatic color change from yellow to blue when CH$_3$CN solutions of [Ru{bpy(C-450)$_4$}$_3$]$^{2+}$ and MV^{2+} were exposed to 460 nm light under deaerated conditions. The blue color was easily identified as MV$^{\bullet+}$ by its characteristic absorption spectrum.[23,24,27,28,37] The existence of a long-lived charge separated species involving the ground-state Ru(III) core and MV$^{+\bullet}$ was immediately ruled out since there was no evidence for the presence of a Ru(III) species in the mixture. In the control experiments, 460 nm photolysis of solutions containing [Ru(dmb)$_3$]$^{2+}$ and MV^{2+} did not produce any observable photochemical products, consistent with complete charge recombination.

(35) The PTZ$^{+\bullet}$ extinction coefficient at 514 nm was estimated from the spectrum provided in ref 31.

(36) Murov, S. L.; Carmichael, I.; Hug, G. L. *Handbook of Photochemistry*, 2nd ed.; Marcel Dekker: New York, 1993; pp 207−208.
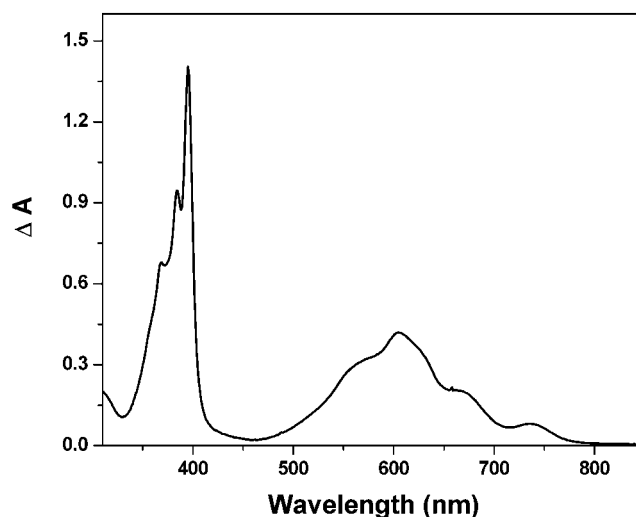
(37) Watanabe, T.; Honda, K. *J. Phys. Chem.* **1982**, *86*, 2617.

There is a major difference between $[Ru(dmb)_3]^{2+}$ and $[Ru\{bpy(C\text{-}450)_4\}_3]^{2+}$ in regards to their oxidative electrochemical behavior which can account for the buildup of $MV^{+\cdot}$ in the latter. The ligand-based irreversible process at $+1.2$ V in $[Ru\{bpy(C\text{-}450)_4\}_3]^{2+}$ is thermodynamically capable of reducing ground-state Ru(III) in the same molecule. This sacrificial process would be facilitated following excited-state oxidative electron transfer, where the ground-state Ru(III) component of the charge-separated pair is thermally reduced by the coumarin-containing ligand structure. The irreversible nature of this reduction process would lead to the accumulation of $MV^{\bullet+}$ since there is no Ru(III) to recombine with. This chemistry also occurred in a control experiment where MV^{2+} was replaced by BV^{2+}. Other than a decrease in the relative efficiency of radical formation, the systems were identical as the $BV^{\bullet+}$ photoproduct accumulated in all samples investigated.[38]

To illustrate similar photochemistry in an appropriate intermolecular model system, the ternary mixture of $[Ru(dmb)_3]^{2+}$, MV^{2+}, and the ligand precursor 3,5-bis(N-(4,6-dimethyl-7-ethylaminocoumarin)methyl)anisole[10,39] (necessary due to poor solubility of $bpy(C\text{-}450)_4$ in CH_3CN) was irradiated with 460 nm light. This photolysis resulted in the accumulation of $MV^{\bullet+}$, presumably derived from the same processes responsible for the buildup of photochemical products in the binary dendritic system. The spectroscopic signature of the $MV^{\bullet+}$ absorption centered at 606 nm illustrates production of the radical.[37] The absorptions below 400 nm were not evaluated due to interference from the large concentration of 3,5-bis(N-(4,6-dimethyl-7-ethylaminocoumarin)methyl)anisole used in the experiment. In the absence of MV^{2+}, 460 nm photolysis of a mixture of $[Ru(dmb)_3]^{2+}$ and the ligand precursor did not produce any permanent absorption changes in the sample, indicating that the C-450 structure is photochemically stable in the absence of oxidative quenchers. Taken together, these observations suggest that 3,5-bis(N-(4,6-dimethyl-7-ethylaminocoumarin)methyl)anisole serves as a intermolecular sacrificial electron donor in the ternary system.

To further probe the proposed sacrificial electron-transfer process in absence of light and oxidative quenchers, $[Ru(dmb)_3]^{3+}$ was prepared.[18,19] On the time scale of our experiments this complex was stable in acidic CH_3CN (H_2SO_4) displaying distinctive absorption bands at 442 and 657 nm (Figure 4). Addition of appropriate reducing agents such as Fe(II) and PTZ led to an immediate color change from green to yellow corresponding to reduction of $[Ru(dmb)_3]^{3+}$ to $[Ru(dmb)_3]^{2+}$, Figure 4.[18] The same effect was observed following the addition of 3,5-bis(N-(4,6-dimethyl-7-ethylaminocoumarin)methyl)anisole, although the process was notably slower. At this time we do not have ability to monitor the dynamics of these processes with stopped-flow kinetics. Qualitatively, these results demonstrate that the $[Ru(dmb)_3]^{3+}$
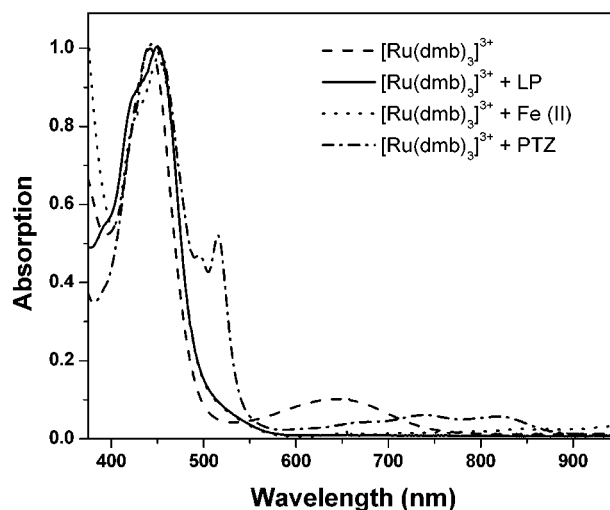

Figure 4. Room-temperature absorption spectra of $[Ru(dmb)_3]^{3+}$ in acidified CH_3CN before (dashed line) and after the addition of 3,5-bis(N-(4,6-dimethyl-7-ethylaminocoumarin)methyl)anisole (LP) (solid line), $FeCl_2$-(aq) (dotted line), and PTZ (dotted−dashed line).

ground-state molecule is thermally reduced by the coumarin-containing dendrimer ligand precursor, consistent with the experimental observations above.

Sequential Intramolecular Sacrificial Electron Transfer. The visible photolysis described above generates at least 9 $MV^{\bullet+}$ species for each $[Ru\{bpy(C\text{-}450)_4\}_3]^{2+}$ present in the solution. These experiments monitored the UV−vis spectrum of the binary mixture $[Ru\{bpy(C\text{-}450)_4\}_3]^{2+}$/$MV^{2+}$(xs) in deaerated CH_3CN as a function of 460 nm photolysis until the production of $MV^{+\cdot}$ was complete. The molar ratio of total viologen radical produced relative to the initial Ru(II) complex was consistently 8.8 ± 0.5, calculated on the basis of the extinction coefficient of the $MV^{\bullet+}$ radical in CH_3CN.[37] In an attempt to elucidate the fate of $[Ru\{bpy(C\text{-}450)_4\}_3]^{2+}$, reversed phase HPLC was employed before and after a 60 min photolysis in the presence of MV^{2+}. Prior to photolysis, the chromatogram displayed MV^{2+} at 6 min and $[Ru\{bpy(C\text{-}450)_4\}_3]^{2+}$ as a distribution of isomers at 35 min. After 460 nm irradiation, $[Ru\{bpy(C\text{-}450)_4\}_3]^{2+}$ was completely consumed and several new species eluted. One clearly defined compound eluted at 19 min (single peak) with an absorption spectrum similar to the coumarin-containing ligand. The other components eluted at various times between 15 and 25 min, most of which displayed absorption spectra similar to that of $[Ru(dmb)_3]^{2+}$. These results indicate that the sequential sacrificial electron-transfer processes within the dendrimer results in substantial bond cleavage yielding "C-450-like" and "$[Ru(dmb)_3]^{2+}$-like" species.

Since the ratio of $MV^{\bullet+}$ formed to initial $[Ru\{bpy(C\text{-}450)_4\}_3]^{2+}$ was consistently 9 to 1, we believe that the bond cleavage occurs in the tertiary amine structures that connect the C-450 units to the aryl ether spacers. If the majority of the bond cleavages occurred between the aryl ether units and the bipyridine structures, we would expect a ratio of $MV^{\bullet+}$ formed to $[Ru\{bpy(C\text{-}450)_4\}_3]^{2+}$ on the order of 6 to 1. Although we cannot completely rule out the latter, the former appears to be more consistent with our observations. Since no permanent photoproducts were observed in related met-

(38) The $BV^{\bullet+}$ extinction coefficient at 608 nm is 14 000 M^{-1} cm^{-1}, as reported in ref 24.
(39) (a) Gilat, S. L.; Adronov, A.; Fréchet, J. M. J. *Angew. Chem., Int. Ed.* **1999**, *38*, 1422. (b) Gilat, S. L.; Adronov, A.; Fréchet, J. M. J. *J. Org. Chem.* **1999**, *64*, 7474.

allo−poly(aryl ether) structures from Balzani's laboratory,[2,9c] we conclude that the bond scission must be occurring in the tertiary amine structures. This is also in line with the fact that sacrificial electron donors can be based upon simple tertiary amine structures such as triethanolamine.[23d,40]

Although a thorough mechanistic study is beyond the scope of this paper, related compounds have been investigated and may give some insight into the current bond cleavage processes.[41−43] Terinary amine electron donors generally lose one electron from the nitrogen lone pair producing a radical cation. This species may undergo back electron transfer, α-carbon deprotonation, or α-carbon σ-bond cleavage. In our system, back electron transfer is not considered. α-Carbon deprotonation generally leads to a strongly reducing carbon-based free radical that may hydrolyze to a secondary amine and a carbonyl compound after electron loss and formation of an intermediate iminium ion.[41−43] α-Carbon σ-bond cleavage initially produces a carbon-based free radical and an iminium ion, both of which continue to perform further chemistry. Although the specific cleavage mechanism is complex and highly dependent on the molecular structure, we believe the dendrimer cleavage process likely follows one of the two general reaction paths outlined above.

The proposed bond cleavage in $[Ru\{bpy(C\text{-}450)_4\}_3]^{2+}$ was indirectly confirmed by fluorescence spectroscopy, Figure 5. Upon UV excitation of the $[Ru\{bpy(C\text{-}450)_4\}_3]^{2+}$ macromolecule, the singlet coumarin fluorescence is nearly quantitatively quenched, and the MLCT-based emission is sensitized.[10] Following the visible photolysis experiments in the presence of MV^{2+}, there is a large increase in coumarin emission (Figure 5a), indicating the C-450 units are no longer quenched by singlet energy transfer to the MLCT core. The excitation spectrum obtained by monitoring the MLCT-based emission ($\lambda_{em} = 610$ nm) also shows that the C-450 units are no longer able to sensitize the emission through singlet energy transfer. This suggests that the core and peripheral molecules are no longer in close proximity, likely a result of bond cleavage, consistent with the HPLC and actinometry data above. The MLCT-based emission spectrum does not shift before and after the photolysis experiments suggesting at the very least that the core complex remains "intact". Scheme 1 summarizes the photochemical processes of $[Ru\{bpy(C\text{-}450)_4\}_3]^{2+}$ in the presence of oxidative quenchers consistent with our experimental observations.

Conclusions

We have detailed a variety of excited-state quenching processes initiated by visible light excitation of a metallo-
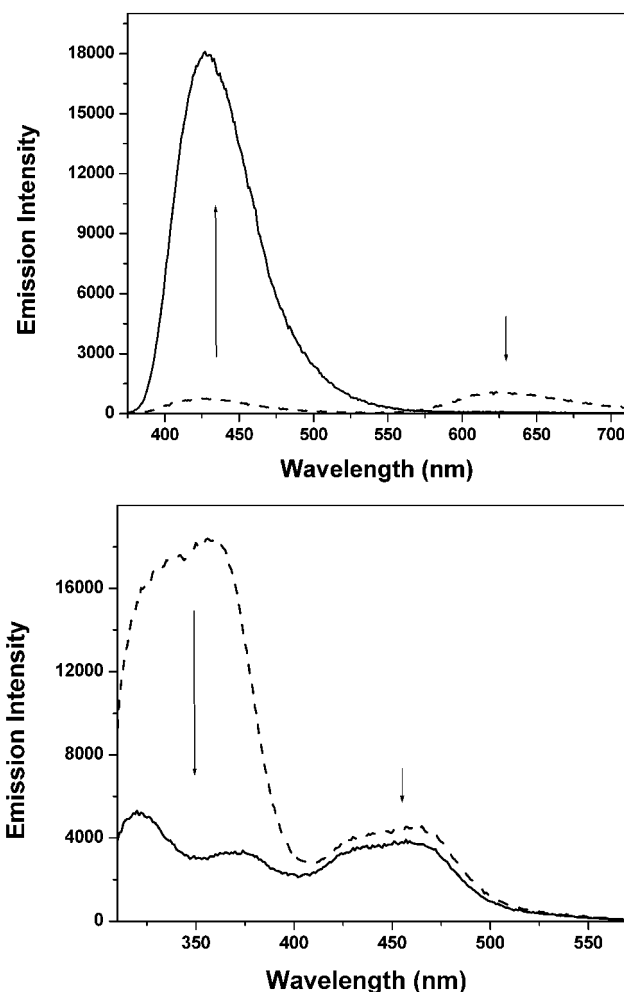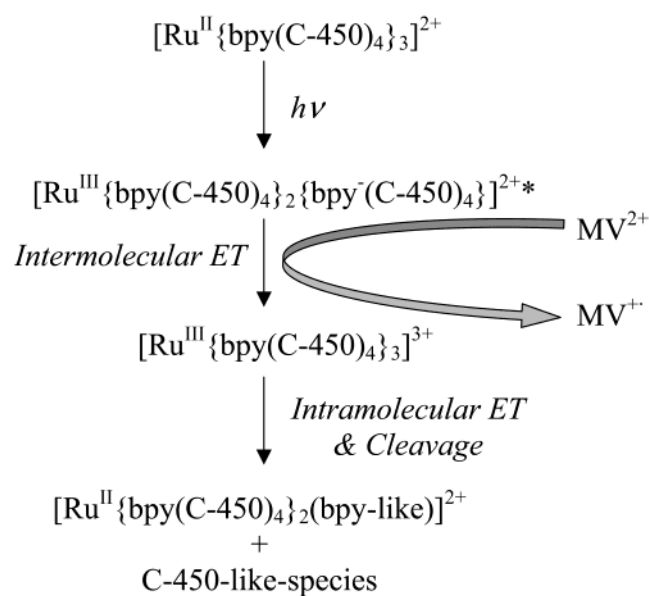

Figure 5. (a) Emission spectra of $[Ru\{bpy(C\text{-}450)_4\}_3]^{2+}$ in the presence of 10 mM MV^{2+} before (dashed line) and after (solid line) 60 min irradiation at 460 nm. The spectra were generated using 360 nm excitation. (b) Excitation spectra of $[Ru\{bpy(C\text{-}450)_4\}_3]^{2+}$ in the presence of 10 mM MV^{2+} before (dashed line) and after (solid line) 60 min irradiation at 460 nm. The emission was monitored at 610 nm.

dendrimer containing a Ru(II) MLCT core that is surrounded by an organic periphery. This microenvironment clearly alters the ground-state electrochemical properties of the redox-active core relative to the $[Ru(dmb)_3]^{2+}$ model compound, shifting the metal-based oxidation to more negative potentials and the first ligand-based reduction to less negative potentials. Although these changes in ground-state potential also affect the excited-state redox potentials making direct comparisons difficult, similar excited-state photochemistry was observed from both compounds. The nearly identical ^{3}MLCT energy of each compound allows quantitative comparison of the triplet energy-transfer rates.

The bimolecular charge-transfer and recombination rates for reductive quenching of the photoactive dendrimer by PTZ were evaluated. These data indicate that the forward process is slightly faster for the dendritic species relative to the model compound and the charge recombination reaction is within experimental error of the diffusion limit. The former is illustrative of electron transfer in the normal region whereas the latter observations are consistent with Rehm−Weller behavior.[23,26,44] In both the forward and reverse PTZ reactions

(40) (a) Surridge, N. A.; McClanahan, S. F.; Hupp, J. T.; Danielson, E.; Gould, S.; Meyer, T. J. *J. Phys. Chem.* **1989**, *93*, 294. (b) Surridge, N.; Hupp, J. T.; McClanahan, S.; Gould, S.; Meyer, T. J. *J. Phys. Chem.* **1989**, *93*, 304.

(41) (a) Gaillard, E. R.; Whitten, D. G. *Acc. Chem. Res.* **1996**, *29*, 292. (b) Haugen, C. M.; Bergmark, W. R.; Whitten, D. G. *J. Am. Chem. Soc.* **1992**, *114*, 10293.

(42) Burton, R. D.; Bartberger, M. D.; Zhang, Y.; Eyler, J. R.; Schanze, K. S. *J. Am. Chem. Soc.* **1996**, *118*, 5655.

(43) (a) Jeon, Y. T.; Lee, C.-P.; Mariano, P. S. *J. Am. Chem. Soc.* **1991**, *113*, 8847. (b) Xu, W.; Zhang, X.-M.; Mariano, P. S. *J. Am. Chem. Soc.* **1991**, *113*, 8863.

Scheme 1

$$[Ru^{II}\{bpy(C\text{-}450)_4\}_3]^{2+}$$

$$\downarrow h\nu$$

$$[Ru^{III}\{bpy(C\text{-}450)_4\}_2\{bpy^-(C\text{-}450)_4\}]^{2+*}$$

Intermolecular ET

MV^{2+}

$MV^{+\cdot}$

$$[Ru^{III}\{bpy(C\text{-}450)_4\}_3]^{3+}$$

Intramolecular ET & Cleavage

$$[Ru^{II}\{bpy(C\text{-}450)_4\}_2(bpy\text{-}like)]^{2+}$$
$$+$$
$$C\text{-}450\text{-}like\text{-}species$$

it is clear that the dendritic architecture has no significant influence on the rates of the electron-transfer processes. Evaluation of photoinduced triplet energy-transfer processes in both systems yield quantitatively similar data, again suggesting that the dendrimer architecture has no apparent effect upon the observed rates.

Quenching by dioxygen and MV^{2+} was attenuated in going from $[Ru(dmb)_3]^{2+}$ to $[Ru\{bpy(C\text{-}450)_4\}_3]^{2+}$. In the case of dioxygen, there is a significant decrease in the quenching rates suggesting the dendrimer structure attenuates the

dioxygen interaction with the core. On the basis of all of the data obtained in the current work, we do not believe that O_2 diffusion to the core is responsible for the attenuation in rate. A more plausible explanation is a reduction in solubility of dioxygen in the vicinity of the metallodendrimer core. For MV^{2+} the slower observed bimolecular rate constant in $[Ru\{bpy(C\text{-}450)_4\}_3]^{2+}$ relative to $[Ru(dmb)_3]^{2+}$ can be largely attributed to the 200 mV difference in driving force. These data support the conclusion that the current metallodendrimer is ineffective in shielding the core from bimolecular chemistry.

Excited-state oxidative electron transfer using MV^{2+} and BV^{2+} acceptors results in the accumulation of viologen radicals and cleavage of the dendrimer peripheral units. These results are consistent with sequential intramolecular sacrificial electron transfer which regenerates the Ru(II) core at least 9 times when MV^{2+} serves as the acceptor.

Supporting Information Available: Figures presenting selected data and analyses used in the determination of rate constants and 77 K emission spectra. This material is available free of charge via the Internet at http://pubs.acs.org.

(44) Rehm, D.; Weller, A. *Isr. J. Chem.* **1970**, *8*, 259.

IC011298C